Conference Paper, Published Version

Kohsrenajad, A.; Rennie, Colin D.

Experimental study of flow field and sediment transport around bridge abutments

Experimental study of flow field and sediment transport around bridge abutments

A. Khosronejad*, and C.D. Rennie**
*Tarbiat Modares University/ Department of Civil Engineering, Tehran, Iran
** University of Ottawa/Department of Civil Engineering, Ottawa, Canada

I. Introduction

A common phenomenon at the bridge site of a river is localized scour around bridge piers and abutments which may cause serious problem for foundations of these structures. The flow field around abutments, which includes flow separation and developing three-dimensional vortex flow, is an extremely complex turbulent flow and the complexity increases with the formation and development of the scour hole. This turbulent flow around the abutments leads to a cone-shape scour hole with a maximum scour depth that depends on the strength of turbulence and vortexes and the flow Froude number. The acceleration and separation of the flow as it moves past the upstream face of the abutment creates a vortex trail that moves downstream in a direction roughly perpendicular to the structure. The result is that the bed around the structure is eroded locally.

The studies on the abutments has been done in two different areas; flow field characteristics and scour hole characteristics near the abutments. Detailed studies of the flow characteristics around the abutment, have been conducted by [1 to 5]. Among these limited studies, the last study [5] is the only one in which the three-dimensional flow field around a vertical–wall and semicircular abutments has been investigated. Regarding the studies of scour hole properties, [6,2,7-9,3] have conducted experimental studies to predict abutment scour hole properties (mainly maximum scour depth) due to different flow conditions.

The present study has two main objectives. First, Measuring and investigating the three-dimensional flow field for two vertical wall semicircular abutments (in front of each other) under clear water regime, using the Acoustic Doppler Velocimeter (ADV). Second, measuring the consequently scour hole characteristics using a digital laser altimeter [10]. Also using a parametric study, the effects of flow conditions such as Froude number, flow discharge, and flow depth on the scour depth has been investigated.

II. Dimensional Analysis

In order to find the effective parameters on the scouring process at an abutment, a dimensional analysis has been performed. Based on the dimensional analysis the maximum non-dimensional scour depth depends on the following non-dimensional parameters (Lim, 1997):

$$\frac{d_s}{h} = f(Fr, F_o, \frac{h}{D}, \sigma_s, K_s) \quad (1)$$

Where d_s is maximum equilibrium scour depth; Fr is flow Froude number; h and D are respectively the flow depth and semicircular abutment diameter; σ_s is geometric standard deviation of the sediment size distribution; K_s is an abutment shape factor; and F_o is sediment densimetric Froude number:

$$F_o = \frac{u}{\sqrt{((S-1)gd_{50})}} \quad (2)$$

Where u is average flow velocity; $S = \rho_s / \rho$ is specific density of sediment particles; ρ_s and ρ are sediment particle density and fluid density, respectively; g is gravitational acceleration; and d_{50} is median diameter of sediment particles by weight.

A parametric analysis on scour process near abutments can be done in terms of the characteristic parameters in equation (1). In this paper, because of the use of only one sediment type and one abutment shape on flume bed, it was clear that the geometric standard deviation of the sediment size distribution and the shape factor of abutments didn't have any effect on the scour depth and scouring process. Hence, a parametric study using the first three non-dimensional parameters on the right hand side of equation (1) has been done.

III. Experimental procedure

Experiments were conducted in a 30 m long, 1.5 m wide and 0.8 m deep laboratory flume in the Civil Engineering Hydraulics Laboratory at the Ottawa University. As illustrated in Figure 1, a movable bed test section was constructed in the flume. The movable bed test section was 7.32 m long, with a recessed 0.25 m deep layer of quasi-uniform non-cohesive sediments with $d_{50} = 0.646$ mm and angle of repose of 42°. The semicircular abutments with a radius of 20 cm were made with a wood core and a stainless steel cover with a

smooth surface. Abutments were embedded in the sediment-bed of the movable portion of flume, and attached to the concrete side-wall of the flume. The flow discharge was measured by a sharp edge rectangular weir installed downstream of the flume. The flow depth was measured by a point gauge with an accuracy of ± 1 mm. The experiments were run under a clear water scour regime for five different inflow discharges. The flow properties related to each experiment are shown in Table 1. The development of scour depth and bed topography was monitored until an equilibrium scour condition was established. The time required to achieve this condition was about 3.5 hours, depending on the flow condition.

After the equilibrium state was achieved, the time-averaged components of flow field velocity in Cartesian coordinate (x, y, z) were measured using a trio of Acoustic Doppler Velocimeters (ADV) operated synchronously. The velocity measurements were taken at two flow depths, one near the free surface and one near the bed, at different sections around the abutment (Figure 2). Because the flow between the two abutments was symmetrical, the measurements were taken between the side wall and centerline of the channel (around one abutment).

Table 1 Flow condition for different runs

Run	Flow Discharge (lit/s)	Inflow velocity (cm/s)	Flow depth (cm)
1	70.0	24.6	19.0
2	58.0	21.4	18.0
3	123.0	36.0	22.8
4	150.3	40.9	24.5
5	131.6	31.0	28.3

The scour depths around the abutment were measured at two different representative perpendicular sections (Peng et al., 2002) with a digital laser altimeter. These two sections (AB and CD) are shown in Figure 3. Also the maximum scour depth (d_s) for each flow condition was measured.

IV. Flow Field

As mentioned above, the flow field was measured in different sections (Figure 2) and at two depths. The measured flow velocities at different depths are shown in Figures (4) to (8). As shown in these figures, close to the abutment the velocity magnitude increases, and the maximum value occurs at the section 4 (the section with maximum constriction in the flow section (Figure (2))) near the edge of abutment. The variation of longitudinal component of velocity shows an increasing trend from upstream toward section 4 and again from section 4 toward downstream it decreases with a maximum at section 4. The transverse velocity component tends to zero at section 4 and its high value occurs at sections of 3 and 5 (see Figure (6)).

This arrangement of flow around abutments leads to three-dimensional vortexes, which are formed at the edge of the abutments and travel downstream roughly in the longitudinal direction (Barbhuya and Dey, 2003).

V. Bed Topography

For all cases in this study (run 1 to 5) the position of maximum scour depth was roughly at the intersection point of lines AB and CD in Figure 3. The greatest scour occurred at this location because the vortexes in this area were the strongest and also the flow velocity and consequently the bed shear stresses in this area were the highest. Figures 9 and 10 show the bed profile along AB and CD lines of Figure (3) for run number 5. As shown in these figures, the maximum scour depth occurs at the intersection of lines AB and CD, and scour depth tend to zero near the centerline of the flume channel.

As seen in Figure 10, the scoured sediments from the scour hole in front of the abutment are deposited at the downstream face of the abutment, where the sediment transport capacity of the flow is reduced (Dongol, 1994).

VI. Parametric Study

The variation of maximum scour depth around abutments versus flow and sediment characteristics in equation (1) has been investigated through Figures (11) to (13). As show in Figure (11) the non-dimensional maximum scour depth (d_s/h) increases linearly with flow Froude number (Fr). A linear regression on these experimental data yields a coefficient of determination (r^2) of 0.94.

Figure (12) shows that the non-dimensional maximum scour depth (d_s/h) also increases linearly with the sediment densimetric Froude number (F_o), with a regression coefficient of determination (r^2) of 0.81 for these data. However, all experimental runs utilized the same sediment, thus (F_o) depended only on flow velocity. Thus, the observed correlation between dimensionless scour depth and (F_o) is due to a linear dependence of scour depth on flow velocity.

The influence of non-dimensional flow depth (h/D) on the non-dimensional maximum scour depth is shown in Figure (13). As can be seen, d_s/h varies non-linearly with non-dimensional flow depth. Again, only one pier diameter was tested in this study. Further, the influence of flow depth is accounted for in the flow Froude number, thus the observed linear relation between dimensionless scour depth and (Fr) is the most meaningful and useful. Several previous studies have utilized flow Froude number to predict abutment scour (see [12] for review).

VII. CONCLUSION

In this study, the flow field and sediment transport around a couple of semicircular abutments have been studied experimentally. The three-dimensional turbulent flow field for five different flow conditions around abutments has been measured using a trio of Acoustic Doppler Velocimeter (ADV) operated synchronously. Depending on the strength of turbulent flow and flow conditions around the abutments, different shapes of bed topography around the abutments emerged. The bed profiles related to five different flow conditions were measured in two perpendicular directions in front of the abutment with a digital laser altimeter. The data of run number 5 for both flow field and bed profile have been depicted in Figures 4 to 10.

Using a parametric approach based on experiments data of five different flows, the effects of non-dimensional water depth, sediment densimetric Froude number and flow Froude number on the maximum scour depth around the semicircular abutments were investigated. The maximum scour depth was linearly related to Froude number.

VIII. REFERENCES

[1] Kwan, T. F., (1984), Study of abutment scour. Rep. No. 328, Scool of Engineering, University of Auckland, Auckland, New Zealand.

[2] Rajaratnam, N., and Nwachukwu, B. A. (1983a). "Flow near groin-like structures." Journal of Hydraulic Engineering, ASCE, 109(3), 463-480.

[3] Lim, S. Y. (1997). "Equilibrium clear-water scour around an abutment." Journal of Hydraulic Engineering, ASCE, 123(3), 237-243.

[4] Ahmed, F., and Rajaratnam, N., (2000) "Observation on flow around bridge abutment", Journal of Hydraulic Engineering, ASCE, Vol. 126, No. 1, pp. 51-59.

[5] Barbhuiya, A. K., and Dey, S., (2003) "Vortex flow field in a scour hole around abutments", International Journal of Sediment Transport Vol. 18, No. 4, pp. 310-325.

[6] Rajaratnam, N., and Nwachukwu, B. A. (1983b). "Erosion near groyne structures." Journal of Hydraulic Engineering, ASCE, 109(3), 463-480.

[7] Kandasamy, J. K., (1989), Abutment scour. Rep. No. 458, School of Engineering, University of Auckland, Auckland, New Zealand.

[8] Melville, B. W., (1992), "Local scour at bridge abutments." Journal of Hydraulic Engineering, ASCE, 118(4), 615-631.

[9] Dongol, D. M. S., (1994), Local scour at bridge abutments. Rep. No. 544. School of Engineering, University of Auckland, Auckland, New Zealand.

[10] Peng, J., Tamai, N., Kawahara, Y. and Huang, W., (2002) "Numerical modeling of local scour around spur dikes", International Journal of Sediment Transport, No. 1, pp. 1-7.

[11] Muntuneau. A., (2004) "Scouring around a cylindrical bridge pier under partially ice-covered flow condition", Master of Science Thesis, Civil Engineering Department, Ottawa University.

[12] Melville, B.W. and S.E. Coleman, 2000, Bridge Scour, Water Resources Publications, Denver, CO."

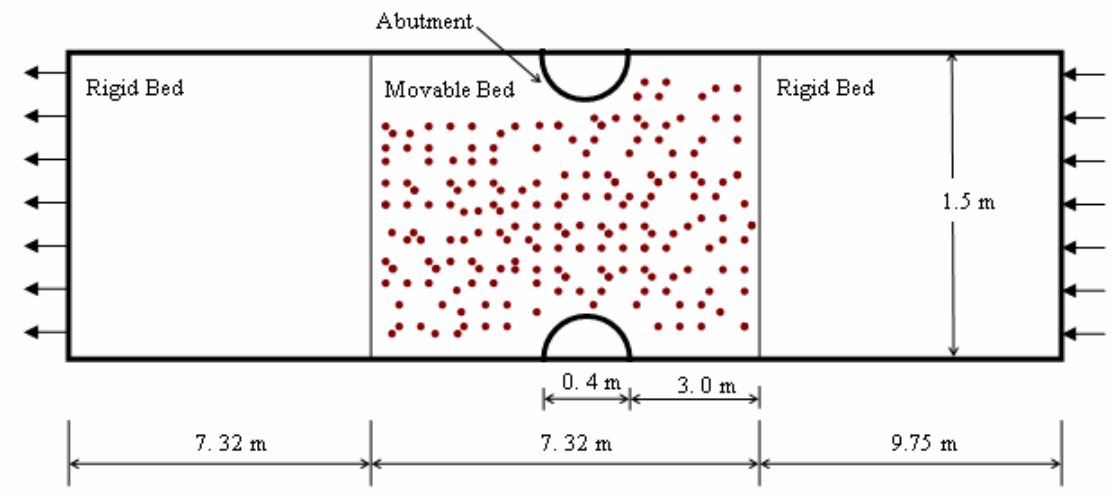

Figure 1 Schematic plan view of the laboratory flume.

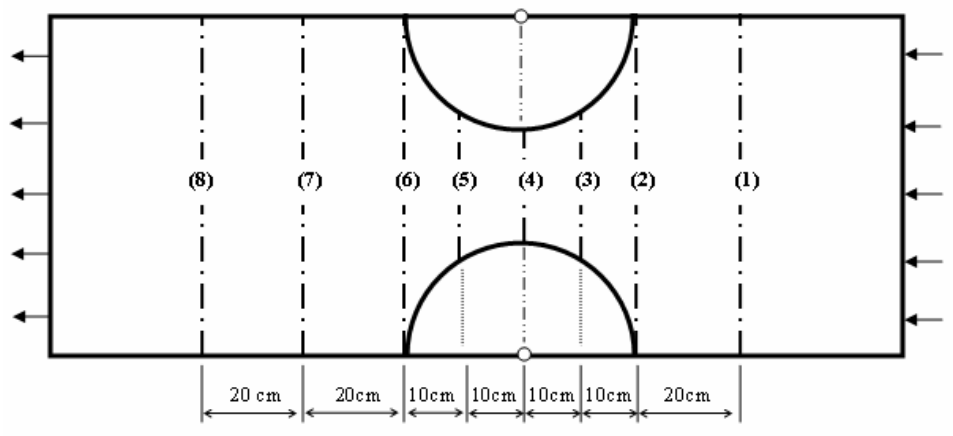

Figure 2 The sections of flow field measurements

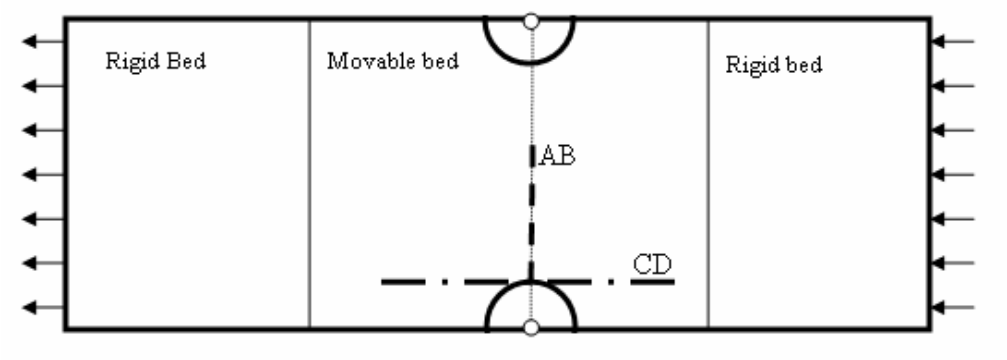

Figure 3 The scour depth measuring sections

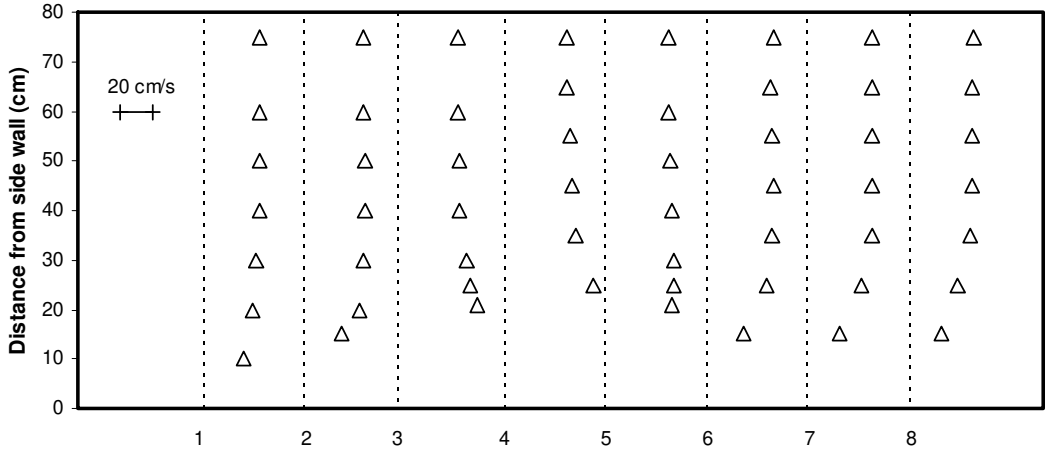

Figure (4) Velocity magnitude in run number of 5 and at the depth of 6.3 cm under free surface for different sections

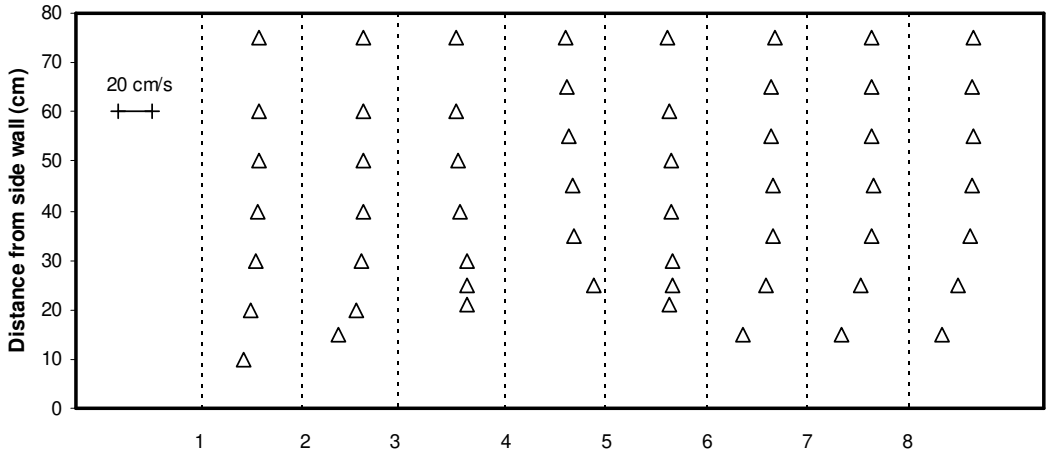

Figure (5) Longitudinal component of velocity in run number of 5 and at the depth of 6.3 cm under free surface for different sections

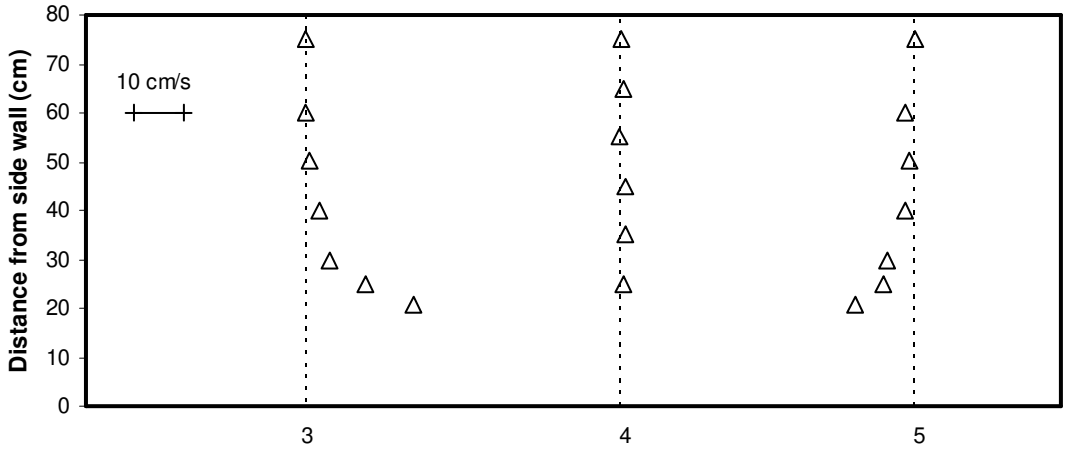

Figure (6) Transverse component of velocity in run number of 5 and at the depth of 6.3 cm under free surface for different sections

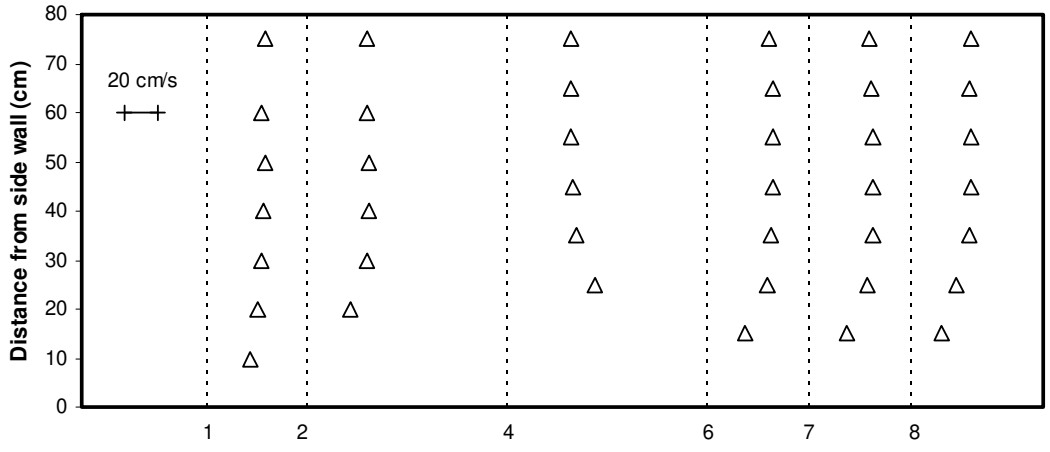

Figure (7) Velocity magnitude in run number of 5 and at a depth 5.0 cm above the bed at different sections

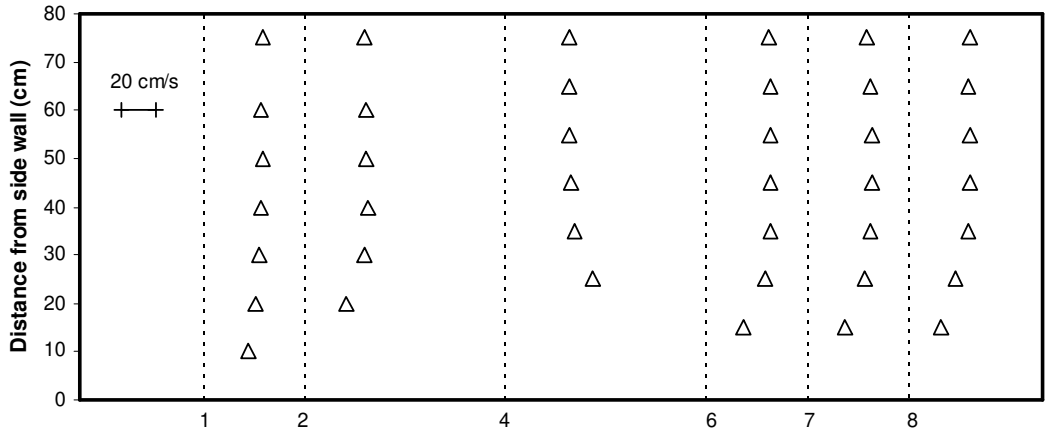

Figure (8) Longitudinal component of velocity in run number of 5 and at a depth 5.0 cm above the bed at different sections

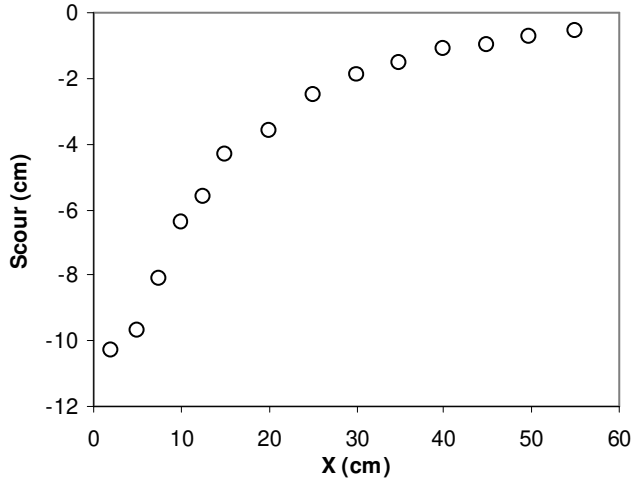

Figure (9) Scour depth and bed profile along AB line for run number 5. The origin is at the intersection of lines AB and CD.

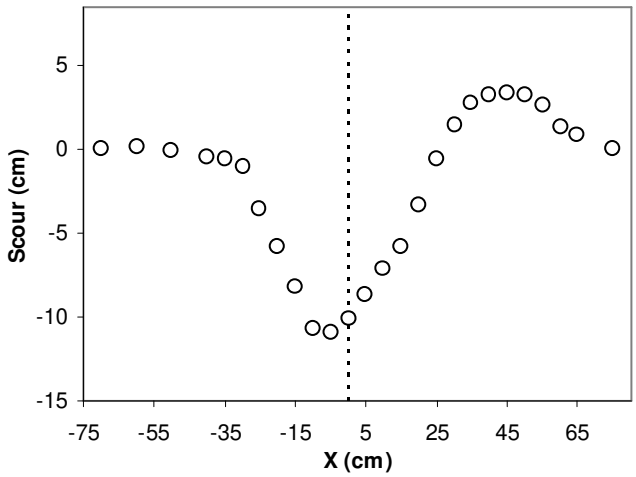

Figure (10) Scour depth and bed profile along CD line for run number of 5 (the dashed line shows the position of intersection point of AB and CD lines)

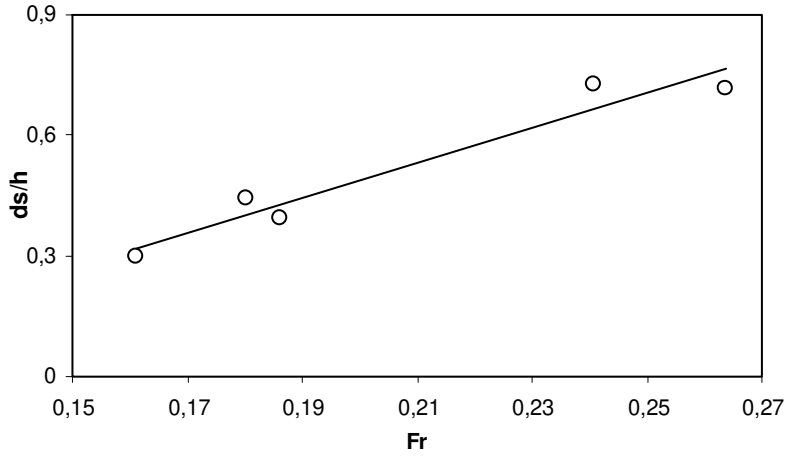

Figure 11 Variation of non-dimensional maximum scour depth versus flow Froude number. Regression equation is $y = 4.3351x - 0.3788$, with $r^2 = 0.94$

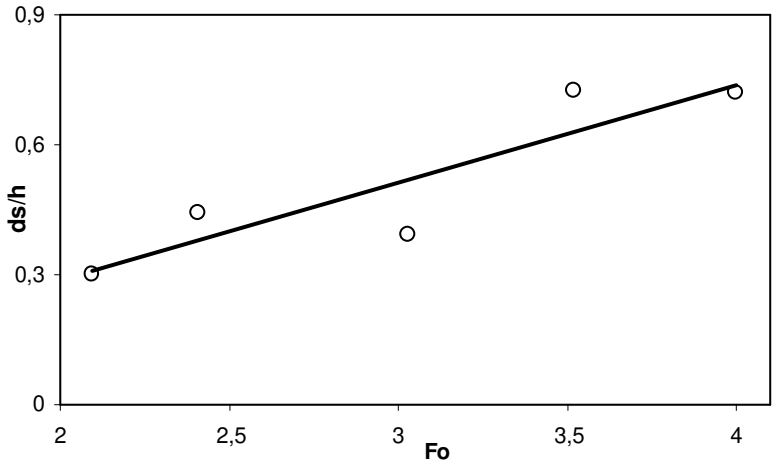

Figure 12 Variation of non-dimensional maximum scour depth versus sediment densimetric Froude number. Regression equation is $y = 22.38x - 0.158$, with $r^2 = 0.81$

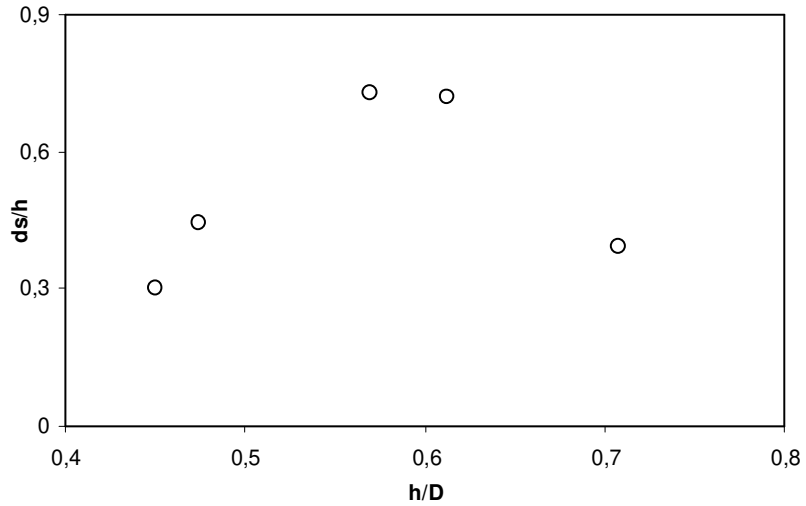

Figure 13 Variation of non-dimensional maximum scour depth versus non-dimensional flow depth.